

## Supplementary Materials

### Catalytic performance of pyrolyzed graphene supported Fe-N-C composite and its application for acid direct methanol fuel cells

Jingjing Xi<sup>a</sup>, Fang Wang<sup>b</sup>, Riguo Mei<sup>b</sup>, Zhijie Gong<sup>a</sup>, Xianping Fan<sup>a</sup>, Hui Yang<sup>a</sup>, Liang An<sup>c</sup>, Qixing Wu<sup>b\*</sup>, Zhongkuan Luo<sup>a,b\*</sup>

<sup>a</sup> Zhejiang California International NanoSystems Institute & Department of Materials Science and Engineering, Zhejiang University, 38 Zhe Da Road, Hangzhou, 310000, China

<sup>b</sup> Shenzhen Key Laboratory of New Lithium-ion Batteries and Mesoporous Materials, College of Chemistry and Environmental Engineering Shenzhen University, 3688 Nanhai Avenue, Nanshan District, Shenzhen, 518060 , China

<sup>c</sup> Department of Mechanical Engineering, the Hong Kong Polytechnic University, Hung Hom, Kowloon, Hong Kong SAR, China

\*Corresponding authors. E-mail address: qxwu@szu.edu.cn (Q.X. Wu) and lzk@szu.edu.cn (Z. K. Luo); Tel: +86-755-26557249; Tax: +86-755-26536141.

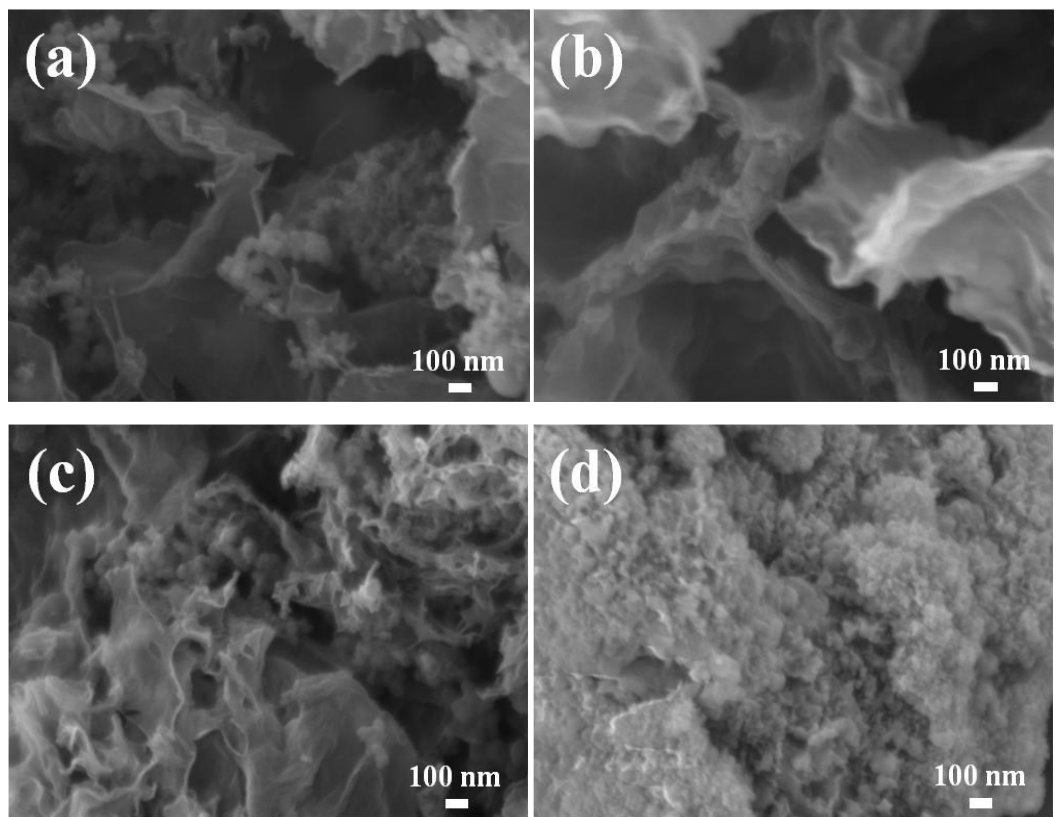


Fig. S1 FESEM images of Fe-N/C/rGO catalysts with different Fe contents of 5 wt % (a), 10 wt % (b) 15 wt % (c) and 20 wt % (d).

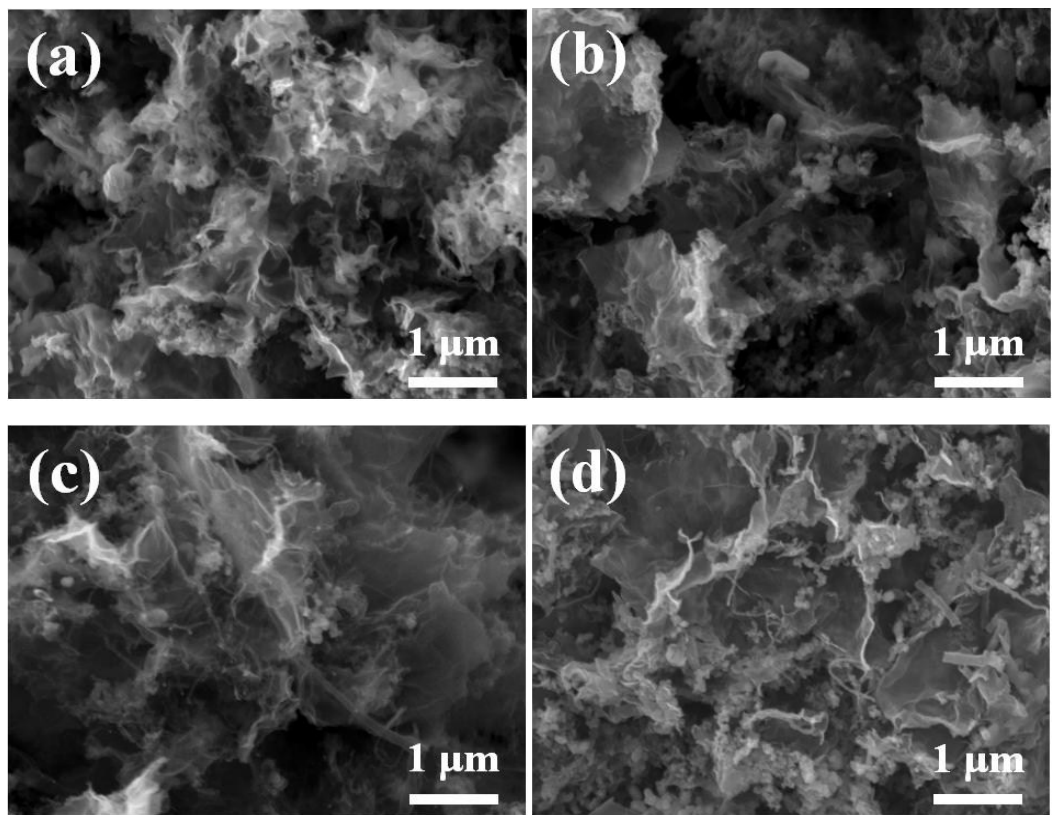


Fig. S2 FESEM images of Fe-N/C/rGO catalysts at different pyrolysis temperatures 650 °C (a), 750 °C (b), 850 °C (c) and 950 °C (d).

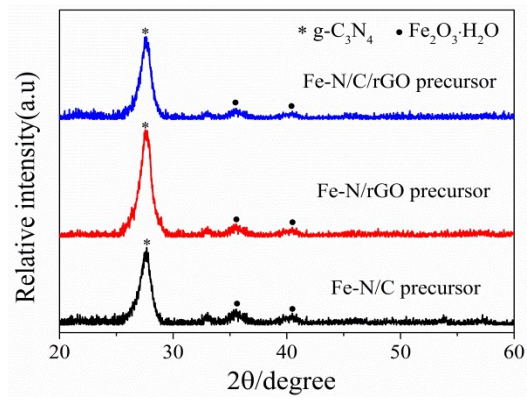


Fig. S3 XRD patterns of Fe-N/C, Fe-N/rGO, Fe-N/C/rGO precursors.

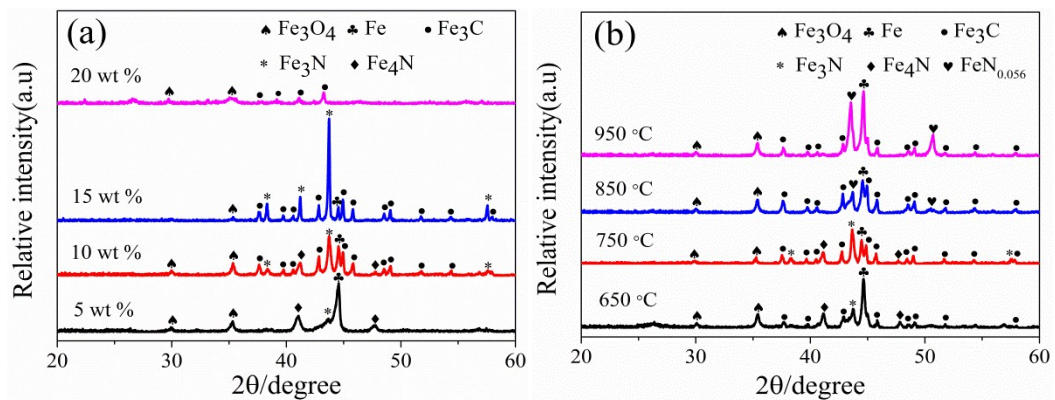


Fig. S4 XRD patterns of Fe-N/C/rGO catalysts with different Fe contents (a) and Fe-N/C/rGO catalysts at different pyrolysis temperatures (b).

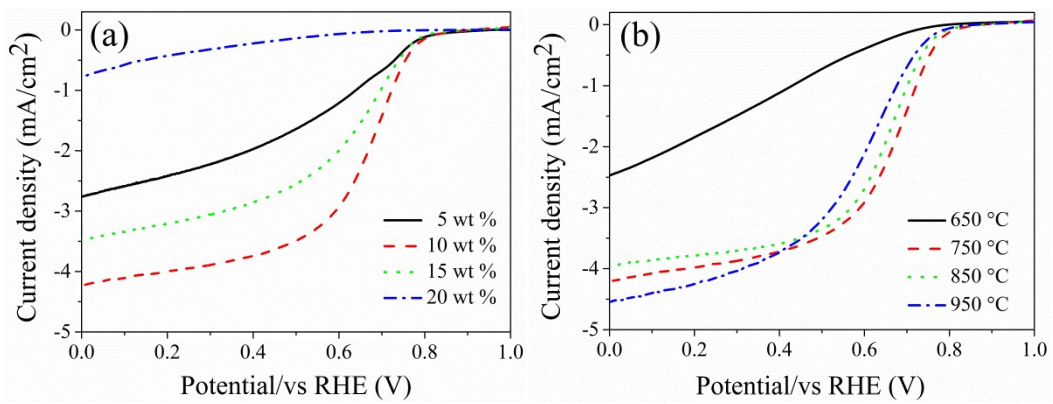


Fig. S5 LSV curves of Fe-N/C/rGO catalysts with different Fe contents (a) and Fe-N/C/rGO catalysts at different pyrolysis temperatures (b) in O<sub>2</sub>-saturated 0.5 M H<sub>2</sub>SO<sub>4</sub> solution at the rotating speed of 1600 rpm and the scan rate of 5 mV s<sup>-1</sup>.

Table S1 Surface areas and pore volumes of Fe-N/C/rGO catalysts with different Fe contents at different pyrolysis temperatures.

Samples	Pyrolysis temperature (°C)	Fe content (wt %)	$S_{\text{BET}}$ ( $\text{m}^2 \text{ g}^{-1}$ )	$V_{\text{pore}}$ ( $\text{cm}^3 \text{ g}^{-1}$ )
Fe-N/C/rGO	750	5	260	0.83
	750	10	256	0.87
	750	15	176	0.25
	750	20	11.6	0.04
	650	10	60.7	0.37
	850	10	214	0.51
	950	10	184	0.46

Table S2 N contents of Fe-N/C/rGO catalysts with different Fe contents at different pyrolysis temperatures.

Samples	Pyrolysis temperature (°C)	Fe content (wt %)	N (wt %)
Fe-N/C/rGO	750	5	6.3
	750	10	5.8
	750	15	4.7
	750	20	3.5
	650	10	20.6
	850	10	3.6
	950	10	2.5

Table S3. Comparison of ORR performance with various Fe-based catalysts in acidic electrolyte.

Sample	$\Delta E_{1/2}$ (mV)*	Scan rate (mV s <sup>-1</sup> )	Rotation rate (rpm)	Current density at 0.4V vs.RHE (mA cm <sup>-2</sup> )	Electrolyte	References
Fe-N/C/rGO-LH	69	5	1600	3.8	0.5 M H <sub>2</sub> SO <sub>4</sub>	This work
Fe/N/C	~200	5	1600	3.3	0.5 M H <sub>2</sub> SO <sub>4</sub>	<i>J. Phys. Chem. C</i> , 2016, 120, 1586–1596
Fe/N/G	~150	10	1600	4.5	0.1 M HClO <sub>4</sub>	<i>Appl. Catal. B-Environ.</i> , 2016, 183, 185–196
Fe-N/MC@0.6	~170	10	1600	4.7	0.1 M HClO <sub>4</sub>	<i>ChemCatChem</i> 2015, 7, 2937-2944
Fe-N/C NNs	108	10	1600	4.05	0.5 M H <sub>2</sub> SO <sub>4</sub>	<i>Sci. Rep.</i> , 2015, 11, 17396
Fe-N/CNN3	~150	10	1600	2.8	0.5 M H <sub>2</sub> SO <sub>4</sub>	<i>Appl. Catal. B-Environ.</i> , 2015, 166–167, 75–83
N-Fe/G(60)-900-S	89	10	1600	5.81	0.1 M HClO <sub>4</sub>	<i>Nanoscale</i> , 2015, 7, 14707–14714
Fe-N-HCMS	150	10	2025	6.5	0.5 M H <sub>2</sub> SO <sub>4</sub>	<i>Adv. Energy Mater.</i> , 2014, 4
Fe-N/C-800	59	10	1600	5.6	0.1 M HClO <sub>4</sub>	<i>J. Am. Chem. Soc.</i> , 2014, 136, 11027–11033

\*  $\Delta E_{1/2}$  represents the difference in the half-wave potentials between Pt/C catalyst and the sample

catalyst, i.e.,  $\Delta E_{1/2} = E_{1/2}(\text{Pt/C}) - E_{1/2}(\text{sample})$ .